Electronic Supplementary Material (ESI) for Chemical Communications

Supporting Information

A phenyl-capped aniline tetramer for Z907/*tert*-butylpyridine-based dye-sensitized solar cells and molecular modelling of the device

Kazuhiro Manseki*[a,b], You Youhai[a,c] and Shozo Yanagida*[a,d]

[a]Center for Advanced Science and Innovation, Osaka University, Yamadaoka 1-1, Suita, Osaka, Japan. [b]Graduate School of Engineering, Environmental and Renewable Energy System (ERES) Division, Gifu University, 1-1, Yanagido, Gifu 501-1193, Japan. *E-mail: kmanseki@gifu-u.ac.jp [c]Centre d Investigacio en Nanociencia i Nanotecnologia (CIN2, CSIC), Campus UAB, Edifici ETSE 2nd Floor. Bellaterra (Barcelona), E-08193, Spain. [d] ISIR, Osaka University,2-1, Mihoga-oka, Ibaraki, Osaka, 567-0047, Japan. *E-mail: yanagida@mls.eng.osaka-u.ac.jp

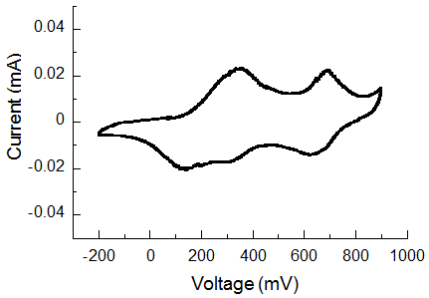

Figure S1 A cyclic voltammogram of 1M H_2SO_4 solution of EPAT. The scanned potential started from 0.9 V to −0.2 V versus saturated Ag/AgCl reference electrode at the scan rate of 100 mV s^{-1}.

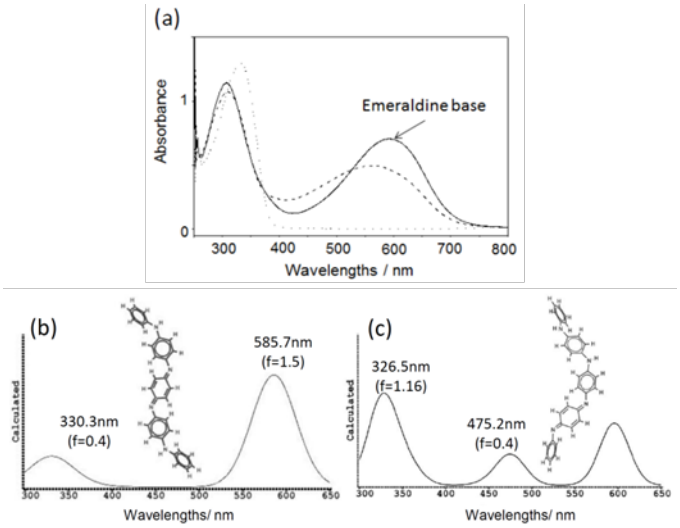

Figure S2 Absorption spectra of phenyl-capped aniline tetramers for four structures, dot: leucoemeraldine-type (LPAT), solid: emeraldine-type (EPAT), dash: pernigraniline-type (PPAT) in DMF solution (a), the DFT-simulated absorption spectra of symmetrical EPAT (b) and

uns

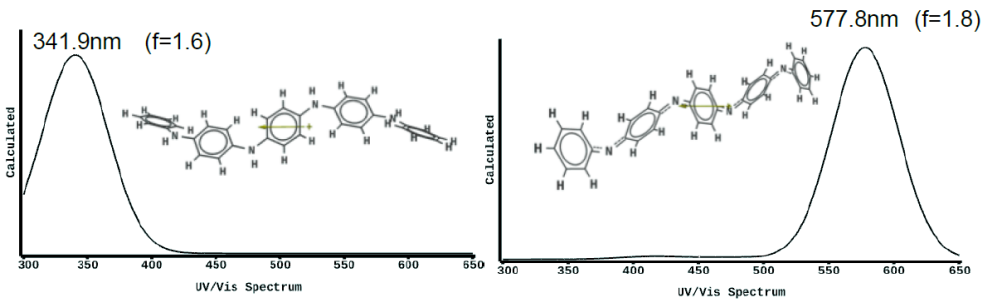

Phenyl-capped Leucoemeraldine base Phenyl-capped Pernigraniline base

Figure S3 Simulated absorption spectra of the phenyl-capped aniline tetramers of leucoemeraldine base and a pernigraniline base determined by DFT calculations. The peaks corresponding to calculated intensity are very consistent with the experimental data. All quantum chemical calculations were performed using DFT at the B3LYP/6-31G(d) level with Spartan '10 package (Wavefunction, Irvine, CA).

Table S1 Total formation energy, HOMO/LUMO energy, and dipole moment for the equilibrium geometries of EPAT, TBP, Z907, N3 (as a substitute of N719), and their associated molecules. Calculations were performed using DFT at the B3LYP/6-31G(d) level with Spartan '10 package.

Name	E (kcal/mol)	E LUMO (eV)	E HOMO (eV)	Dipole (debye)
EPAT (symmetrical)	−863841.90	−2.51	−4.72	0.06
EPAT (unsymmetrical)	−863841.19	−2.55	−4.73	3.74
TBP	−254481.03	−0.46	−6.75	2.79
EPAT&TBP(H-bonding)	−1118331.87	−2.34	−4.47	5.71
EPAT&TBP (H-π stacking)	−1118326.12	−2.44	−4.67	2.53
Z907	−1977723.59	−2.88	−4.52	16.6
N3(N719)	−1770316.66	−3.22	−4.82	14.85

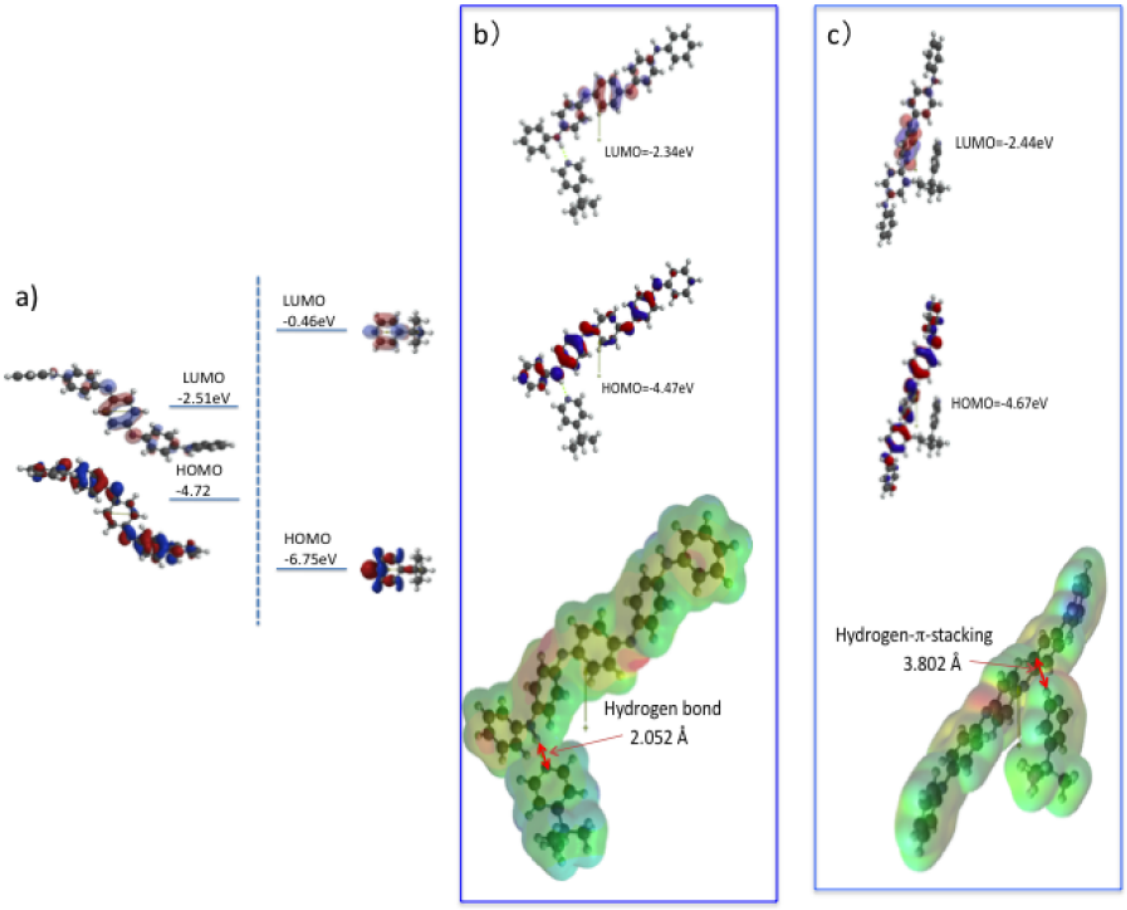

Figure S4 Energy relationship and shape of the frontier orbitals of EPAT, TBP (a) and energy structures of two kinds of associated EPTA and TBP, and electrostatic potential map and specific distances for the associated EPAT/TBP molecules through hydrogen bonding (b) and through weak hydrogen-π stacking bond (van der Waals bond) (c).

Table S2 Total formation energy, HOMO/LUMO energy, and dipole moment for the equilibrium geometries of EPAT, *n*-nonane, *n*-nonylbenzene, *n*-nonane/EPAT, Z907, *n*-nonylbenzene/EPAT, and Z907/EPAT.

Name	E (kcal/mol)	E LUMO (eV)	E HOMO (eV)	Dipole (debye)
EPAT (symmetrical)	−863841.9	−2.51	−4.72	0.06
n−Nonane	−222782.71	2.47	−7.96	0.05
n−Nonylbenzene	−367769.05	0.16	−6.37	0.36
n−C_9H_{19}/EPAT	−1086626.08	−2.57	−4.76	1.51
n−C_9H_{19}−C_6H_5/EPAT	−1231613.35	−2.5	−4.68	0.99
Z907	−1977723.59	−2.88	−4.52	16.6
Z907/EPAT(symetrical)	−2841574.84	−3	−4.59	15.22

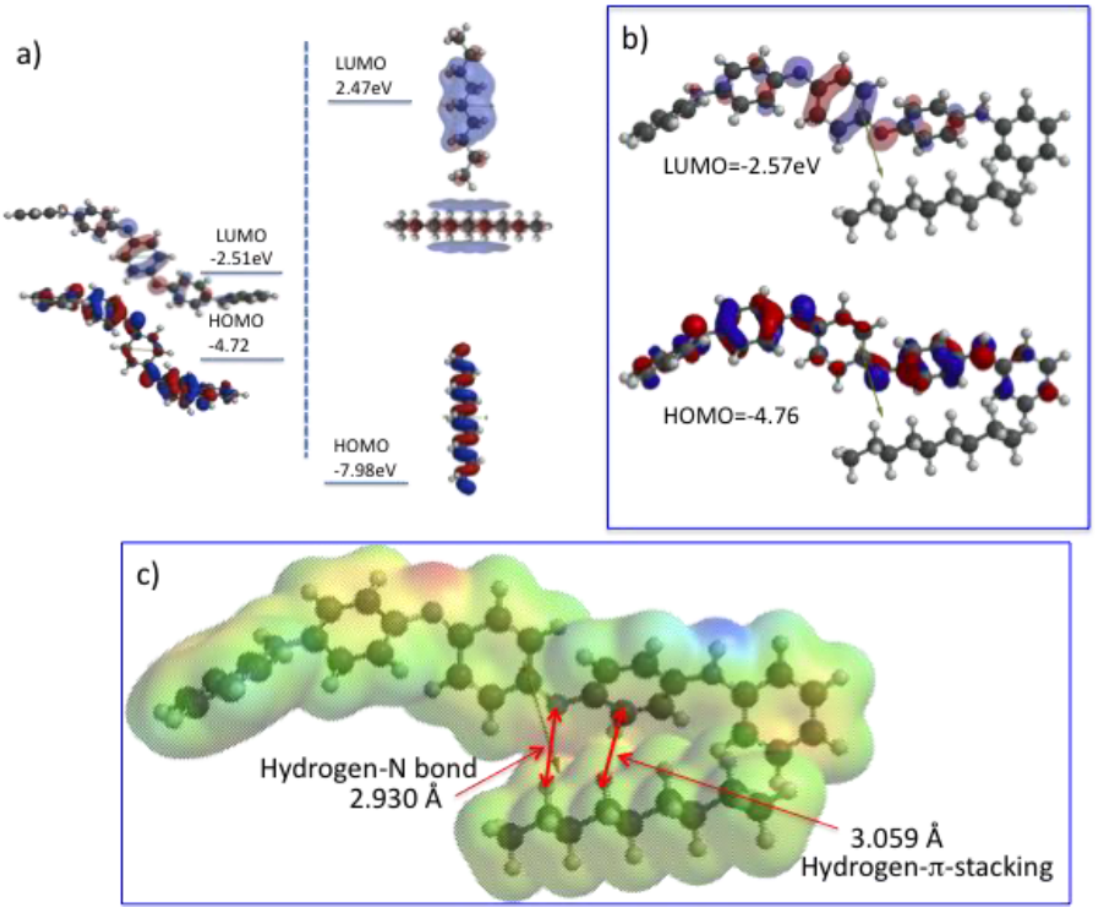

Figure S5Energy relationship and shape of the frontier orbitals of EPAT and *n*-nonane (a), and the energy structure of the associated EPAT/n-nonane, (b) and the electrostatic potential map and specific non-bonded distances for the associated EPAT/*n*-nonane molecules (c).

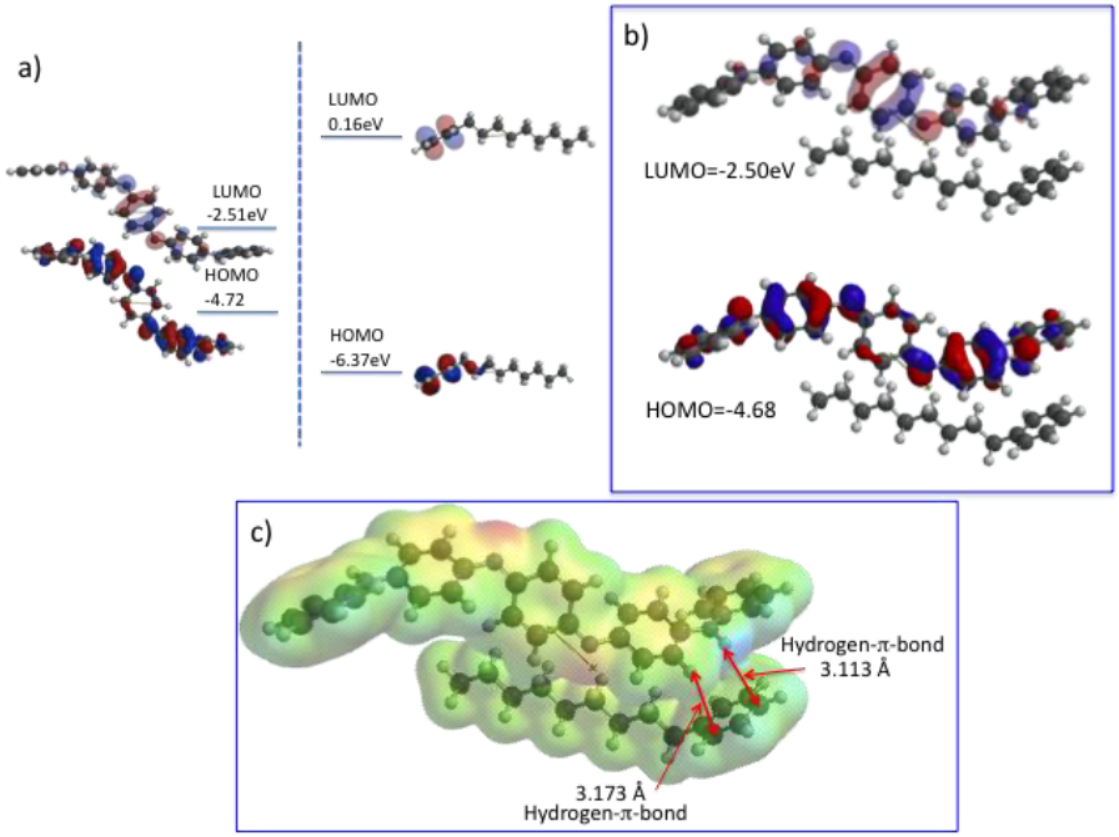

Figure S6 Energy relationship and shape of the frontier orbitals of EPAT and *n*-nonylbenzene (a), and the energy structure of the associated EPAT/ *n*-nonylbenzene, (b), the electrostatic potential map and specific non-bonded distances for the EPAT/*n*-nonylbenzene molecule (c).

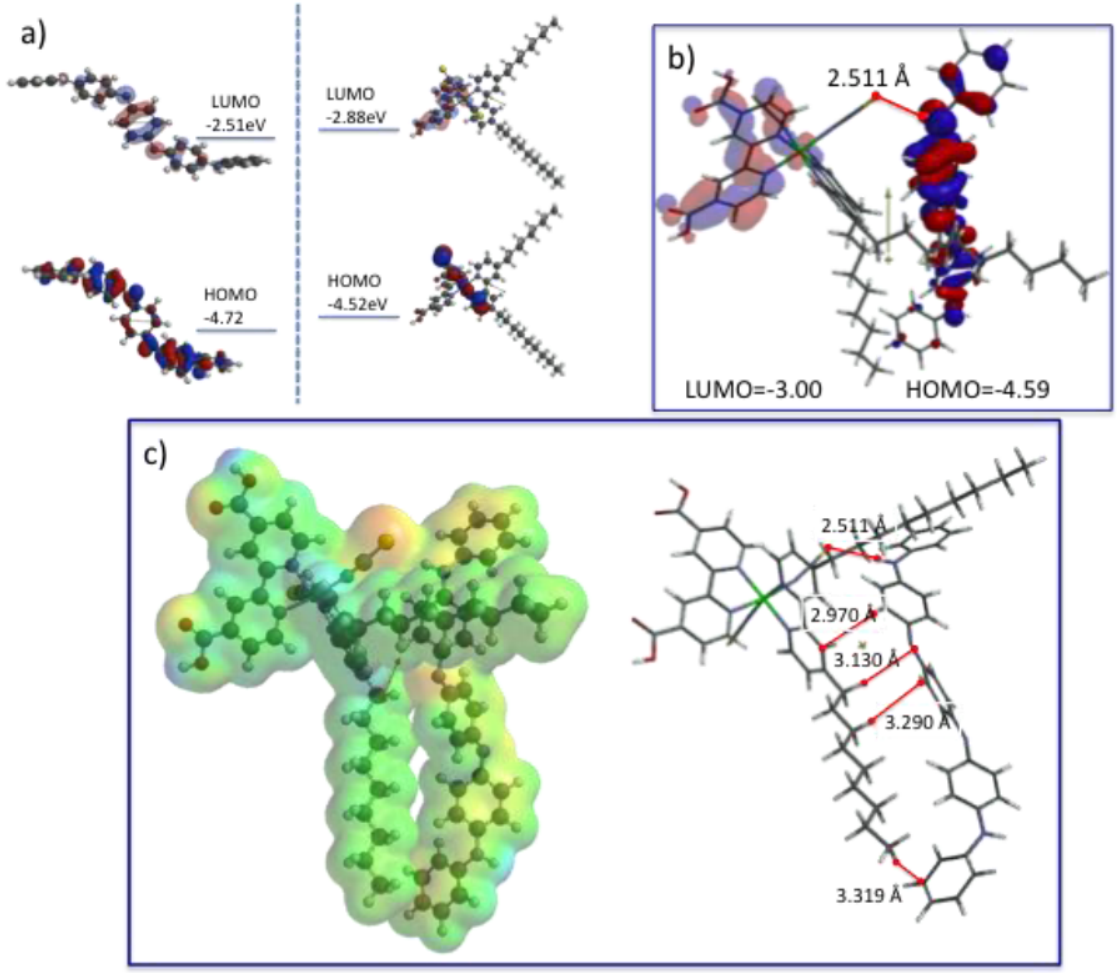

Figure S7 Energy relationships of the frontier orbitals between EPAT and Z907 (a), and the energy structure of the associated EPAT/Z907 (b), the electrostatic potential map and specific non-bonded distances for the EPAT/Z907 molecule through sulfur of SCN and hydrogen-bond, and hydrogen-π stacking bonds (c).

Experimental

Materials

4-Tert-butylpyridine (TBP), guanidinium thiocyanate (GSCN) dodecylbenzenesulfonic acid (DBSA), were obtained from Aldrich and used as received. Acetonitrile, *tert*-butyl alcohol and valeronitrile were purchased from Fluka and used as received.

Fabrication of nanoporous-TiO_2 electrodes[1]

The FTO glass (4 mm thickness, Nippon Sheet Glass, SnO_2: F, 10 ohm/sq) was first cleaned in a detergent solution using an ultrasonic bath for 10 min., and then rinsed with water and ethanol. The FTO glass plates were then immersed into a 40 mM aqueous $TiCl_4$ solution at 70 °C for 30min. and washed with water and ethanol. A layer of TiO_2 paste (PST-18NR, particle size, 18 nm, CCIC in Japan) was coated on the FTO glass plates by screen-printing (screen printing machine: AISI304, plane weaving, 150 mesh, Mesh Industrial Co., Ltd., Japan) and then dried for 6 min. at 125 °C. This screen-printing procedure with the paste (PST-18NR) was repeated to control the film thickness (measured by a profiler, Sloan, Dektak3). After drying the films at 125 °C, the paste of PST 400C (particle size, 400 nm, CCIC in Japan) was deposited by the screen-printing method, resulting in the light-scattering TiO_2 layer containing the anatase particles of 3–4 μm thickness. The electrodes coated with the TiO_2 pastes were sintered at 500 °C for 15 min. The TiO_2 films were treated with the 40mM $TiCl_4$ solution at 60°C and were rinsed with water and ethanol, followed by the sintering at 500 °C for 30 min. After cooling to 80 °C, the TiO_2 electrodes were immersed into the 5.0×10^{-4} M dye solution of acetonitrile and *tert*-butylalcohol (volume ratio, 1:1) in which electrodes were kept at room temperature for 24 h. to complete the sensitizer uptake.

Preparation of counter Au-electrodes

Au was deposited on the FTO glass by using the ion sputter coater (Eiko IB-3, Eiko Engineering Co., Ltd, Japan).

Electrolyte

The electrolyte consists of the solution of 0.04 M phenyl-capped aniline tetramer (emeraldine base), 0.08 M DBSA, 0.1 M GSCN and 0.5 M TBP in valeronitrile.

DSC assembly

The dye-coated TiO_2 electrodes and Au-counter electrodes were assembled into a sandwich type cell and sealed by using thermal adhesive films (HIMILAN, Mitsui-Dupont Polychemical, 35 μm of thickness). The size of the TiO_2 electrodes was

0.235 cm^2. The electrolyte was introduced into the cell via vacuum backfilling. Finally, the hole was sealed using a thermal adhesive film (HIMILAN, Mitsui-Dupont Polychemical, 35 μm of thickness) and a cover glass (0.1 mm thickness).

Measurements

The power conversion efficiency of DSCs was recorded using a PC controlled voltage-current source meter (R6246, Advantest) under a solar simulator illumination (Yamashita Denso,YSS-80) of air mass 1.5 (100mW·cm^{-2}) at 25 °C. The incident light intensity was 100 mW·cm^{-2} calibrated with a standard Si solar cell. Cyclic voltammetry (CV) measurement was performed on a Bas100W electrochemical system. UV-vis spectra were recorded on a SHIMADZU UV-3101PC spectrometer.

Reference

1. S. Ito, T. N. Murakami, P. Comte, P. Liska, C. Grätzel, M. K. Nazeeruddin, M.Grätzel, *Thin Solid Films* **2008**, 516(14), 4613.